Advanced optimization strategies for integrated dynamic process operations

Lorenz T. Biegler

Department of Chemical Engineering, Carnegie Mellon University, Pittsburgh, PA 15213, United States

ARTICLE INFO

ABSTRACT

Modern approaches for dynamic optimization trace their inception to Pontryagin's Maximum Principle 60 years ago. Since then the application of large-scale nonlinear programming strategies has been extended to deal with challenging real-world process optimization problems. This study discusses and demonstrates the effectiveness of dynamic optimization on three case studies on real-world chemical processes. In the first case, we consider the optimal design of runaway reactors, where simulation models may lead to unbounded profiles for many choices of design and operating conditions. As a result, optimization based on repeated simulations typically fails, and a simultaneous, equation-based approach must be applied. Second, we consider optimal operating policies for grade transitions in polymer processes. Modeled as an optimal control problem, we demonstrate how incorporation of product specification bands leads to multi-stage formulations that greatly improve process performance and significantly reduce off-grade product. Third, we consider an optimization strategy for the integration of scheduling and dynamic process operation for general continuous/batch processes. The method introduces a discrete time formulation for simultaneous optimization of scheduling and operating decisions. Finally, we provide a concise summary of directions and challenges for future extension of these optimization formulations and solution strategies.

© 2017 Elsevier Ltd. All rights reserved.

1. Introduction

The study of dynamic optimization problems originates from the rich field of the *Calculus of Variations*, treated in a number of classical texts including Bliss (1946) and Courant and Hilbert (1953). The evolution of variational calculus to the more general field of *optimal control* stems from Pontryagin's maximum principle discovered in the 1950s (Boltyanskii et al., 1956; Pontryagin et al., 1962). Optimal control has led to a broad set of applications ranging from aeronautical applications (Bryson and Ho, 1975; Raghunathan et al., 2004; Betts, 2010; Arrieta-Camacho and Biegler, 2006), robotics (Büskens and Maurer, 2001; Steinbach et al., 1997), and process control (Ray, 1981). Here we consider the impact of optimal control in the design, operation and integration of chemical process systems. Specifically, reactor design requires the dynamic optimization of differential-algebraic equation models to deliver efficient and safe operation within operating and product constraints. Moreover, dynamic operations occur in both batch and continuous processes. For the latter case, optimal transitions are needed to handle the dynamics of product grade changes, cyclic operations, catalyst deactivation over time, and fouling of heat transfer surfaces in a production cycle. For batch processes, optimal operating recipes need to be generated for dynamic operation of batch units. These batch units also need to integrate to the overall plant and to an operating cycle with interactions to other processes over broader length scales, as well as planning, scheduling and control tasks that span several time scales.

In the next section we introduce the statement of the dynamic optimization problem and review a number of approaches to solve this problem, with a focus on the simultaneous collocation approach and a summary of its characteristics and advantages. The next three sections demonstrate the power of the simultaneous approach on three real-world examples. Section 3 focuses on optimal reactor design with runaway reactions. We present an optimization study on graded bed reactors and demonstrate why the simultaneous method is successful, while other methods fail. Section 4 considers dynamic operations of continuous operations and focuses on optimal grade transition of a polymer process with detailed models for molecular weight distributions. Here the simultaneous approach leads to a multi-stage formulation that leads to significant reductions in off-spec product and faster grade transitions. Section 5 considers the integration of batch processes with
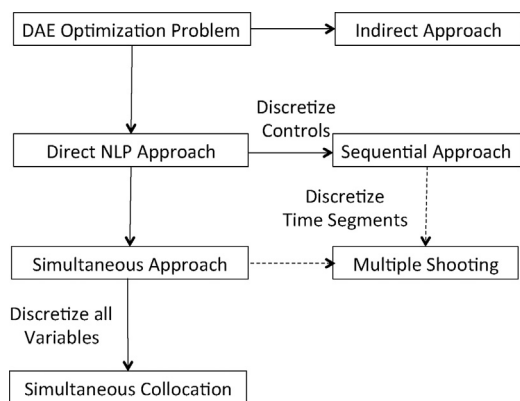
E-mail address: biegler@cmu.edu

Fig. 1. Solution strategies for dynamic optimization.

the logistics of scheduling and interactions with other units. Here we present an optimization study that links the generation of optimal operating recipes together with a resource task network formulation for the production of multiple products in an overall plant. Finally, conclusions and directions for future work are given in the last section.

2. Dynamic problem statement

We consider the optimization problem stated in the following form:

$$\min \quad \Phi(z(t_f)) \tag{1a}$$

$$s.t. \quad \frac{dz}{dt} = f(z(t), y(t), u(t), p), \tag{1b}$$

$$z(0) = z_0(p)$$

$$g_E(z(t), y(t), u(t), p) = 0 \tag{1c}$$

$$g_I(z(t), y(t), u(t), p) \leq 0 \tag{1d}$$

$$h_E(z(t_f)) = 0, \quad h_I(z(t_f)) \leq 0 \tag{1e}$$

The variables in this optimization problem are the *time-independent parameters p* as well as *differential state variables z(t)*, *algebraic variables y(t)*, *control variables u(t)*, which are functions of the scalar $t \in [t_0, t_f]$. As constraints we have differential and algebraic equations (DAEs) given by (1b) and (1c) and we assume without loss of generality that this DAE system is index one.

As shown in Fig. 1, a number of approaches can be taken to solve Problem (1). DAE optimization problems are solved using a variational approach or by various strategies that apply nonlinear programming (NLP) solvers to the DAE model. Until the 1970s, these problems were solved using an *indirect* or *variational approach*, based on the necessary conditions for optimality obtained from Pontryagin's Maximum Principle (Pontryagin et al., 1962; Bryson and Ho, 1975). For problems without inequality constraints, these conditions can be written as a set of DAEs. Obtaining a solution to these equations requires careful attention to the boundary conditions. Often the state variables have specified initial conditions and the adjoint variables have final conditions; the resulting two-point boundary value problem (TPBVP) can be addressed with different approaches, including single shooting, invariant embedding, multiple shooting or some discretization method such as collocation on finite elements or finite differences. On the other hand, if the problem requires the handling of active inequality constraints, finding the correct switching structure as well as suitable initial guesses for state and adjoint variables is often very difficult. Early approaches to deal with these problems can be found in Bryson and Ho (1975).

Methods that apply NLP solvers can be separated into two groups, *sequential* and *simultaneous* strategies. In the *sequential methods*, also known as *control vector parameterization*, only the control variables are discretized. In this formulation the control variables are represented as piecewise polynomials (Vassiliadis et al., 1994a,b; Barton et al., 1998) and optimization is performed with respect to the polynomial coefficients. Given initial conditions and a set of control parameters, the DAE model is embedded within an inner loop controlled by an NLP solver. Parameters (p) that represent the control variables are updated by the NLP solver itself. Gradients of the objective function with respect to the control coefficients and parameters are calculated either by direct sensitivity equations derived from the DAE system or by integration of the adjoint equations; several codes have been developed for both sensitivity methods.

Sequential strategies are relatively easy to construct and to apply, as they incorporate the components of reliable DAE and NLP solvers. On the other hand, repeated numerical integration of the DAE model is required, which may become time consuming for large scale problems. However, optimal control problems with many degrees of freedom lead to expensive (direct) sensitivity calculations required by the NLP; they also retain calculation noise from the DAE integrator and their expense dominates the computation cost. Moreover, sequential approaches are known to fail on unstable dynamic systems (Ascher and Petzold, 1998; Flores-Tlacuahuac et al., 2005). Finally, state constraints can be handled only approximately by sequential methods, within the limits of the control parameterization.

Multiple shooting is a simultaneous approach that inherits many of the advantages of sequential approaches. Here the time domain is partitioned into smaller time elements and the DAE models are integrated separately in each element, along with corresponding sensitivity equations (Bock, 1983; Bock and Plitt, 1984; Leineweber, 1999). Control variables are parametrized as in the sequential approach and gradient information is obtained for both the control variables and the initial conditions of the states variables in each element. Finally, equality constraints are added to the NLP to link the elements and ensure that the states are continuous across each element. As with the sequential approach, inequality constraints for states and controls can be imposed directly at the grid points, and care is needed to avoid noisy and expensive sensitivity calculations.

Finally, in the *Simultaneous Collocation Approach*, we discretize both the state and control profiles in time using collocation of finite elements. This approach corresponds to a particular implicit Runge–Kutta method with high order accuracy and superior stability properties. Also known as fully implicit *Gauss* forms, these methods can be expensive (and not widely applied) as initial value solvers. However, for boundary value problems and optimal control problems, this approach is essential and also requires far fewer time steps to obtain accurate solutions. On the other hand, simultaneous collocation leads to large-scale NLP problems, which may require efficient optimization strategies (see Betts, 2010; Biegler, 2010). Because simultaneous collocation methods directly couple the solution of the DAE system with the optimization problem, the dynamic system is solved only once, at the optimal point. Intermediate solutions that do not exist, become unstable or require excessive computational effort are therefore avoided. Coupled with modern NLP solvers and optimization environments, this approach can be considerably more efficient than sequential methods on large-scale problems.

The simultaneous collocation approach has a number of advantages over other approaches to dynamic optimization. First, when control variables are discretized at the same level as the state variables, the Karush Kuhn Tucker (KKT) conditions of the simultaneous NLP are consistent with the optimality conditions of the discretized variational problem (Biegler, 2010). Moreover, under

general assumptions, convergence properties to the optimal control solution of (1) have been analyzed (Cuthrell and Biegler, 1989; Hager, 2000) and extended to Radau collocation (Kameswaran and Biegler, 2008a,b).

Second, as with multiple shooting approaches, simultaneous approaches can deal with instabilities that occur for a range of inputs. Because they are extensions of robust boundary value solvers, they are able to "pin down" unstable modes (i.e., increasing modes in the forward direction). This property has important advantages for problems that include transitions to unstable points, optimization of chaotic systems (Bock and Plitt, 1984) and systems with limit cycles and bifurcations, as illustrated in Flores-Tlacuahuac et al. (2005).
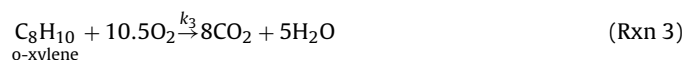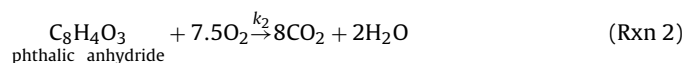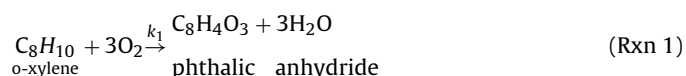
Finally, simultaneous collocation methods also allow the direct enforcement of state and control variable constraints, at the same level of discretization as the state variables of the DAE system. As discussed in Biegler (2010), these present some interesting advantages on large-scale problems. Moreover, simultaneous collocation approaches have demonstrated distinct advantages for singular control problems and problems with high index path constraints (Betts and Campbell, 2003; Kameswaran and Biegler, 2008a,b; Chen and Biegler, 2016).

Nevertheless, simultaneous collocation often requires the application of large-scale optimization solvers (e.g., CONOPT (Drud, 1994), IPOPT (Wächter and Biegler, 2006), KNITRO (Byrd et al., 2000)) and optimization modeling environments (e.g., GAMS (Brooke et al., 1998), AIMMS (AIMMS, 2014), AMPL (Fourer et al., 2002) and Pyomo (Hart et al., 2012)).

3. Optimal design for graded bed reactors

Optimization of packed bed catalytic reactors with runaway reactions represents an important challenge for dynamic optimization. In order to increase productivity and prevent temperature profiles from becoming unbounded, graded (or zoned) bed techniques introduce nonuniform active catalyst distributions along the reactor bed, with catalysts diluted with inerts in different compositions. The catalyst dilution strategy can also improve dynamic controllability of the reactor under constrained cooling capacities.

In Nie et al. (2013a,b) a systematic design approach was developed for graded bed optimization with nonuniform catalytic activity distributions. This study considers the vapor phase oxidation of o-xylene to phthalic anhydride with vanadium pentoxide catalyst. Typically, o-xylene is mixed with excess air before entering the reactor. The highly exothermic reaction scheme can be summarized as follows:

$$C_8H_{10} + 3O_2 \xrightarrow{k_1} \underset{\text{phthalic anhydride}}{C_8H_4O_3 + 3H_2O} \qquad \text{(Rxn 1)}$$
$$\underset{\text{o-xylene}}{}$$

$$\underset{\text{phthalic anhydride}}{C_8H_4O_3} + 7.5O_2 \xrightarrow{k_2} 8CO_2 + 2H_2O \qquad \text{(Rxn 2)}$$

$$\underset{\text{o-xylene}}{C_8H_{10}} + 10.5O_2 \xrightarrow{k_3} 8CO_2 + 5H_2O \qquad \text{(Rxn 3)}$$

Reaction rates are modeled as pseudo-first-order and proportional to a catalyst activity profile $\sigma(V) \in [0, 1]$ that varies along the bed length V. The reactor model is formulated in both radial and axial directions and a novel *alpha model* was applied in Nie et al. (2013a,b) to transform mass and energy balances to DAEs in the axial coordinate. The optimization problem is to maximize the productivity of

Table 1
Optimization statistics for increasing catalytic zones.

Zone # N	Product rate [kg/(m³ h)]	T_{max} [K]	CPU [s]
1	79.33	684.58	19.2
2	100.32	669.82	16.0
4	106.50	676.76	20.3
10	106.63	679.38	29.2
∞	106.64	680	2798.91

phthalic anhydride at the reactor outlet. Key product specifications are given as end-point constraints:

$$\text{Selectivity}: \frac{f_{PA}^o}{f_{OX}^i - f_{OX}^o} \geq 75.0\%$$

$$\text{Conversion}: \frac{f_{OX}^i - f_{OX}^o}{f_{OX}^i} \geq 92.5\%.$$

where f_{PA}^o is outlet molar flow rate of phthalic anhydride, and f_{OX}^i / f_{OX}^o are inlet/outlet molar flow rates of o-xylene. In addition to $\sigma(V)$, the decision variables include inlet temperature T^i, wall temperature T^c and inlet flow rates f_j^i, with feed composition fixed.

The reactor optimization takes the form of Problem (1), and a sequential approach would treat the reactor model as a *black box*, where the state trajectories (and their sensitivities required in optimization search) are provided by external numerical DAE solvers. This method relies heavily on repeated solution of DAEs. However, when decisions are chosen so that temperature profiles become unbounded, as with any unstable system, the DAE solver fails, the optimization strategy aborts, and the user is left to "pick up the pieces."

In contrast, the *simultaneous collocation* approach incorporates the DAEs as constraints directly within the NLP. Because the temperature and composition profiles are bounded in the optimization problem, the simultaneous approach can handle unstable DAE systems as boundary value problems, and it ensures convergence to the optimal catalyst distribution problem with runaway reactions.

Moreover, the graded bed problem is a singular optimal control problem, as control variables appear only linearly in (1) and the optimal control policy cannot be explicitly recovered from the stationary conditions. As degrees of freedom increase numerical optimization methods often give rise to highly oscillatory profiles, especially when a high-resolution discretization scheme is used for the control variables. One way to avoid this behavior is to use a coarse discretization and to design a graded bed with only a few catalytic zones with constant σ values. The multi-zone optimization formulation is introduced by dividing the reactor bed into $N(\geqslant 1)$ catalytic zones, with varying segment length, and the activity coefficient σ as a piece-wise constant function over the bed length.

The optimization model, discretized with 3 point collocation over 60 finite elements, was solved with IPOPT 3.10 on an Intel Core i7 CPU, with an increasing number of zones N, in order to inspect the influence of finer zoning on the production of phthalic anhydride. The optimization formulation with over 7800 variables and constraints solves to local optimality for all cases, and the results and model statistics are listed in Table 1. Higher productivity is achieved by raising both the mass flow and cooling temperature, and (for $N > 1$) the maximum temperature remains bounded by 680 K through manipulation of the graded beds.

As seen from Table 1, a single uniform bed ($N = 1$) has the lowest productivity. Additional activity zones show significant improvement, but with steadily diminishing benefits. Fig. 2 shows profiles with 4 to 10 zones. With $N = 10$ the dilute zones, between the first and last upper bound segments, approximate a *singular arc* with a
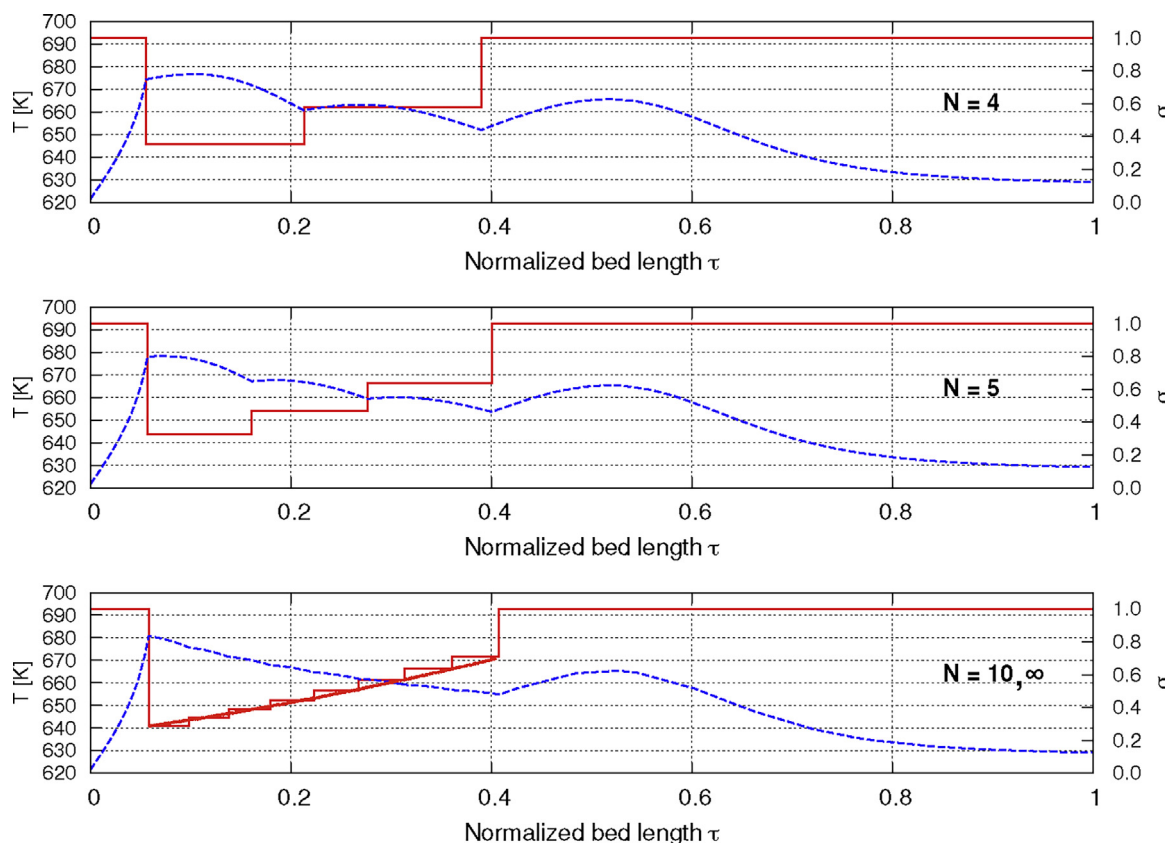
Fig. 2. Optimal temperature $(T(\tau))$ and catalyst dilution $(\sigma(\tau))$ profiles of the multi-zone beds $N = 4, 5, 10, \infty$.

shallow response surface that has little additional influence on the optimal objective function value.

To obtain a limiting solution that captures the singular arc as $N \to \infty$, we note an increased ill-conditioning of the NLP. A recent approach that avoids this problem, and leads to solutions of singular arcs are given in Chen and Biegler (2016). In addition to solving the discretized optimal control problem, optimality conditions from the infinite dimensional problem (1) must be strictly enforced; finite elements are adjusted and added in order to improve the approximation error on these conditions. The resulting approach in Chen and Biegler (2016) leads to a bilevel optimization formulation where the inner NLP solves the discretized problem with fixed elements, while the (smaller, but more nonlinear) outer problem manages the finite elements, in order to satisfy Euler–Lagrange Conditions on the singular controls to a numerical tolerance. Applying this approach to the graded bed reactor optimization leads to the temperature and activity profiles given in Fig. 2. This verified singular control solution has similar performance as with $N = 10$ but with considerable increase in computational cost.

4. Integrated optimal grade transitions with product specification bands

This section considers the development of optimization models for the grade transition of polyethylene solution polymerization processes. Among the large family of polyethylene products, linear low-density polyethylene (LLDPE) is among the most versatile, and is widely manufactured and marketed. Typically made by copolymerization of ethylene with longer-chain olefins and single-site catalysts, LLDPE has a narrower distribution of molecular weight and leads to various product grades defined by specified product properties such as melt index (MI) and density. These product grades are typically produced on the same production line, and

grade transitions are frequently applied. Consequently, grade transitions require the minimization of off-spec product as well as loss of production time, while meeting operating and safety constraints.

In the solution polymerization process shown in Fig. 4, LLDPE is produced in a loop reactor operating at high recycle ratio that can be modeled as an ideal CSTR. Ethylene, comonomer, catalyst, hydrogen, solvent and impurities are continuously injected into the jacketed reactor, and ethylene is partially polymerized to produce products of different grades. Cooling media flow through the reactor jacket to control the reactor temperature to an acceptable range, and to ensure all components remain in liquid phase. The reactor is followed by a separator, which separates polymers from other components and a splitter which recycles both liquid and vapor streams. For grade transition optimization, available manipulated variables include ethylene flowrate, comonomer flowrate, hydrogen flowrate, catalyst flowrate and inlet cooling media temperature; controlled variables are ethylene conversion, MI and product density. Within the process, a detailed reactor model has been created that includes a moment model that allows product quality to be incorporated directly into the optimization problem. This reactor model considers a single-site catalyst and the reactions in Table 2. Here, P_0 is the empty site; M, monomer and comonomer denoted by different subscripts i and j; $P_{n,i}$, growing polymer of chain length n and end-group M_i; $D_{n,i}$, dead polymer of chain length n and end-group M_i; C_d, dead catalyst site; and A, S, T, X for cocatalyst, solvent, transfer agent and poison, respectively.

4.1. Multi-stage grade transition

Grade transition optimization can be formulated as Problem (1) and specific grade transition optimization problems are typically formulated as "point to point" problems where the objective is to minimize time or resources consumed. This is denoted as a single

Table 2
LLDPE polymerization reactions from Shi et al. (2016a,b).

Chain initiation	$P_0 + M_i \Rightarrow P_{1,i}$
Chain propagation	$P_{n,i} + M_j \Rightarrow P_{n+1,j}$
Chain transfer	
1. To hydrogen	$P_{n,i} + H_2 \Rightarrow P_0 + D_{n,i}$
2. To cocatalyst	$P_{n,i} + A \Rightarrow P_0 + D_{n,i}$
3. To solvent	$P_{n,i} + S \Rightarrow P_0 + D_{n,i}$
4. To transfer agent	$P_{n,i} + T \Rightarrow P_0 + D_{n,i}$
5. To monomer	$P_{n,i} + M_j \Rightarrow P_{1,j} + D_{n,i}$
6. Spontaneous	$P_{n,i} \Rightarrow P_0 + D_{n,i}$
Chain deactivation	
1. By poison	$P_{n,i} + X \Rightarrow Cd + D_{n,i}$
	$P_0 + X \Rightarrow C_d$
2. Spontaneous	$P_{n,i} \Rightarrow C_d + D_{n,i}$
	$P_0 \Rightarrow C_d$

stage optimization, starting from the current product specifications and operating conditions at t_0 and moving to the target specifications and operating conditions at some unknown t_f. The dynamic optimization problem is defined by:

$$\min \quad \int_{t_0}^{t_f} \|y(t) - y^*\|_Q^2 + \frac{1}{\gamma}\|u(t) - u^*\|_R^2 dt$$
$$s.t. \quad \text{Reactor Moment model} \qquad (2)$$
$$\text{Process Model equations}$$
$$\text{Process constraints}$$

where $y(t)$, y^* are output variables and corresponding target, $u(t)$, u^* are input variables and corresponding target, and Q and R are scaling matrices. Full details on this model are provided in Shi et al. (2016a,b). In the objective function, the first term addresses the gap between current property predictions and their targets, while the second is a regularization term that ensures that the target steady state is reached smoothly. When this regularization term is removed, the problem becomes an ill-conditioned, singular control problem, where solution profiles are highly sensitive to numerical error. As the regularization weight $1/\gamma$ increases, smoother control profiles can be observed at the expense of longer transition time.

To leverage the flexibility of simultaneous solution strategies, the dynamic optimization can be formulated as a "set to set" transition problem, leading to a multi-stage formulation where the objective excludes parts of the transition that satisfy product specification bands. The result is that transition time and off-grade product are significantly reduced. This multi-stage optimization problem for minimum transition time is written as:

$$\min \quad \alpha_t(t_2 - t_1) + \beta_t(t_1 - t_0)$$
$$+ \int_{t_0}^{t_f} \|y(t) - y^*\|_Q^2 + \frac{1}{\gamma}\|u(t) - u^*\|_R^2 dt$$
$$s.t. \quad \text{Reactor Moment Model}$$
$$\text{Process Model Equations}$$
$$\text{Process Constraints} \qquad (3)$$
$$\text{Property Specifications in 1st and 3rd Stages}$$
$$MI_{A,\min} \leq MI \leq MI_{A,\max},$$
$$\rho_{A,\min} \leq \rho \leq \rho_{A,\max}, t \in [t_0, t_1]$$
$$MI_{B,\min} \leq MI \leq MI_{B,\max},$$
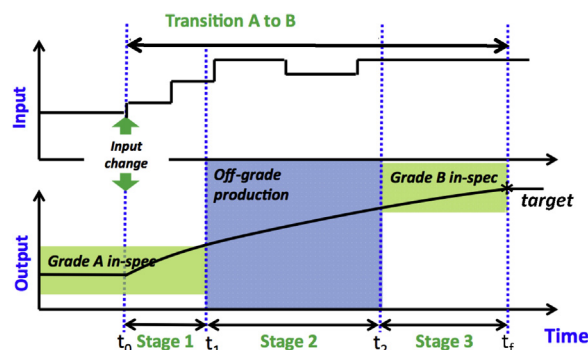$$\rho_{B,\min} \leq \rho \leq \rho_{B,\max}, t \in [t_2, t_f]$$

Fig. 3. Grade transitions when specification bands are considered.

Moreover, the multi-stage formulation is easily modified for direct minimization of off-grade material, by substituting the corresponding objective.

$$\alpha_p \int_{t_1}^{t_2} P(t)dt + \beta_t(t_1 - t_0) + \int_{t_0}^{t_f} \|y(t) - y^*\|_Q^2$$
$$+ \frac{1}{\gamma}\|u(t) - u^*\|_R^2 dt \qquad (4)$$

Here $P(t)$ is production rate at time t, and off-grade product is made in time period $[t_1, t_2]$. Similar to the case with minimum transition time, the weights α_p, β_t and γ can be tuned systematically with fixed Q and R.

4.2. Single-stage vs. multi-stage results

A sketch of the multi-stage evolution is shown in Fig. 3. In the above objective function, the terms represent the time period of producing off-grade product $(t_2 - t_1)$, initiation to the first transition $(t_1 - t_0)$ and a regularization term that promotes a smooth solution to the target steady state of the second grade, respectively. α_t, β_t, γ, Q and R are weighting factors which are tuned to balance these objectives.

Note that the grade transition problem considers not just the individual reactor, but the dynamic optimization of the entire plant with liquid and vapor recycles. This also requires consideration of longer time horizons for the grade transition. In addition, constraints are imposed to maintain the reactor in liquid phase over the entire operation. These constraints require detailed vapor-liquid equilibrium models to determine bubble point limits of the reacting mixture over time. Finally, to approximate the transport delay in the recycle streams, a variable time delay has been built into the model in order to accommodate the dynamics of the grade transition problem.

The optimization problems (2)–(4) directly minimize transition times, off-grade production times and off-grade product, respectively. Detailed presentation of results and comparison of the resulting dynamic optimization cases is given in Shi et al. (2016a,b). To compare the single-stage and multi-stage results, we consider the grade transition from high density A ($\rho = 0.908$, $MI = 1.0$ g/10 min) to low density B ($\rho = 0.864$, $MI = 12.0$ g/10 min) product. Four different grade transition policies are compared for this particular transition: (a) step response from steady state of A to B, (b) single-stage formulation (2), (c) multi-stage formulation with minimum transition time (3) and (d) multi-stage formulation modified for minimum off-grade production instead of minimum time (4). With 3 point collocation and 48 finite elements, the resulting NLPs contain 157,000 variables and constraints and require from 2 to 11 CPU minutes to solve.

The optimal profiles of product density are shown in Fig. 5 with product property specification bands marked by horizontal
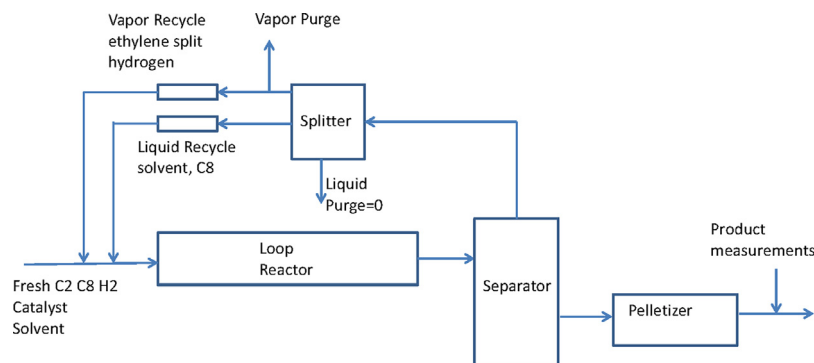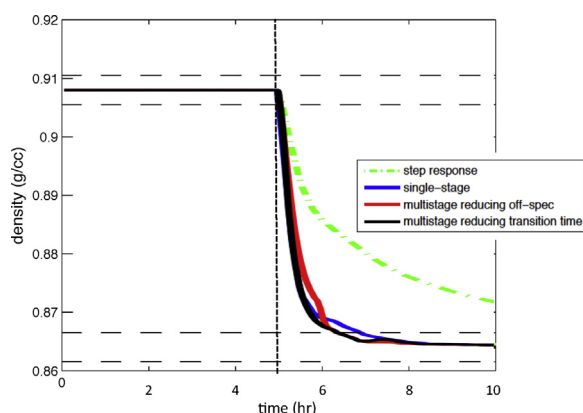
Fig. 4. Flowsheet of Solution polymerization process.

Fig. 5. A→B: Comparison of density profiles and accumulated off-grade production with four grade transition policies with $t_0 = 5$.

Fig. 6. Robust optimal transition strategy with back-off constraints.

dashed lines; additional input and output profiles can be found in Shi et al. (2016a,b). Included in this figure is the straightforward step response to target steady state as a typical base case. As shown in Table 3, the single stage optimization reduces off-grade production and transition time by an order of magnitude over the step response case. The multi-stage optimization provides the best transition policies and reduces off-grade production and transition time by an additional 30%. Starting at $t_0 = 5$ h the multi-stage transition quickly leaves the first specification band at t_1, performs a fast transition to the boundary of the second band and reaches Stage 3 at $t_2 = 6.36$ h. In contrast, t_1 is about the same for the single-stage solution, but this solution reaches the boundary of the target band at $t_2 = 6.91$ h. Similarly, the modified multi-stage formulation (4) directly minimizes off-grade production and has significantly lower off-grade production during transition. Consequently, multi-stage formulations significantly outperform the single stage formulation, and are able to directly reduce the amount of off-grade product as well as transition time.

4.3. Optimal grade transition under uncertainty

The optimal grade transitions in Fig. 5 show significant performance improvements with perfectly known models under nominal conditions. However, this performance can deteriorate in the presence of uncertainties, disturbances and model mismatch, leading to a huge impact on feasible process operation. To extend the dynamic optimization to handle uncertainty, Shi et al. (2016a,b) apply the concept of back-off constraints to represent the uncertainty description and provide a safety margin for the process constraints and grade specifications. This approach leads to a problem formulation that does not increase the size of the optimization problem, and is supported by Monte Carlo simulations, under which back-off constraint margins are evaluated. A sketch of the back-off approach is shown in Fig. 6 and detailed information in the optimization strategy is provided in Shi et al. (2016a,b).

To address model uncertainties in the grade transition model (4), robust optimization formulations with constant and time-varying back-off terms were constructed and demonstrated in Shi et al. (2016a,b) on the above LLDPE process, with quite favorable process performance and no additional complexity in the optimization. Moreover, the deployment of *time-varying back-off constraints* leads

Table 3
A→B: Comparison of step response, single-stage and multi-stage solutions for transition to low density.

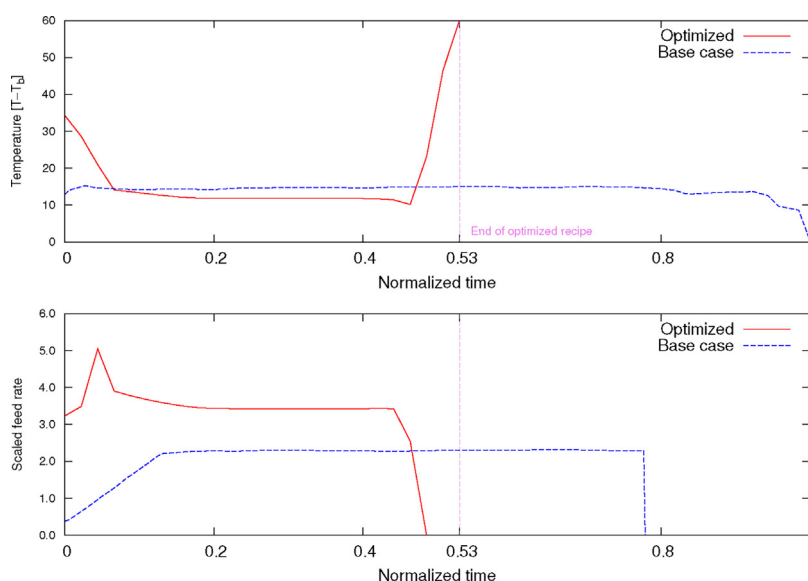| A→B	$t_3 - t_0$ (h)	$t_1 - t_0$ (h)	$t_2 - t_1$ (h)	off-grade prod. (scaled)
Step response	>20	0.18	>20	>8.96
Single-stage	1.91	0.04	1.87	1.00
Min-off-grade	1.31	0.10	1.21	0.61
Min-time	1.28	0.10	1.18	0.65

Fig. 7. Optimal control profiles of the process.

to much less conservative transition policies. In particular, with kinetic parameter uncertainties, the back-off constrained approach leads to slightly longer transition times (typically with less than an additional 20%) over nominal optimal cases. In addition, under uncertainty these policies effectively avoid infeasible operations due to violation of product specifications and operating constraints.

5. Integration of dynamic operations with scheduling

Integrated optimization of production schedules and unit control strategies is a promising approach to improve plant profitability. Bhatia and Biegler (1996) were among the first to incorporate rigorous dynamic models into batch scheduling problems. While that study was restricted to flowshop plants with limited transfer polices, their work showed great potential of the integrated optimization approach to improve plant profitability. Nyström et al. (2005) studied a grade sequencing and transition problem of a polymerization process, where the transition trajectories, operating points, and sequencing of grades are determined all-at-once with a mixed integer dynamic optimization formulation. Cost minimization is achieved by reducing raw material use and off-grade products.

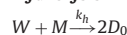### 5.1. Polyol polymerization case study

This section considers an integrated optimization of a semi-batch process for the manufacture of polyether polyols. A general-purpose formulation was developed in Nie et al. (2015a,b) to integrate scheduling and dynamic optimization for batch/continuous processes. For the polyether polyol process, we first developed a rigorous mathematical reactor model based on the reaction scheme described in Table 4 (Nie et al., 2013a,b). This dynamic model is based on first-principles including mass and population balances, reaction kinetics and vapor–liquid equilibria. A dynamic optimization problem is then formulated to minimize the processing time within target requirements, along with additional requirements on product quality and process safety. In particular, novel constraints are imposed over time to reflect limitations on cooling duty as well as an adiabatic temperature rise constraint that enforces safe operation even if cooling is lost.

Solved by the simultaneous collocation strategy we obtain optimal temperature and monomer addition profiles in Fig. 7.
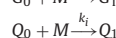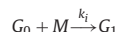
Table 4
Reactions for polyol polymerization. G_n denotes growing product chains of length n, D_n denotes dormant product chains of length n, Q_n denotes growing by-product chains of length n, R_n denotes dormant by-product chains of length n.
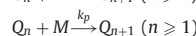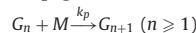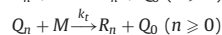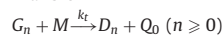
Hydrolysis

$$W + M \xrightarrow{k_h} 2D_0$$

Initiation

$$G_0 + M \xrightarrow{k_i} G_1$$

$$Q_0 + M \xrightarrow{k_i} Q_1$$

Propagation

$$G_n + M \xrightarrow{k_p} G_{n+1} \ (n \geqslant 1)$$

$$Q_n + M \xrightarrow{k_p} Q_{n+1} \ (n \geqslant 1)$$

Transfer

$$G_n + M \xrightarrow{k_t} D_n + Q_0 \ (n \geqslant 0)$$

$$Q_n + M \xrightarrow{k_t} R_n + Q_0 \ (n \geqslant 0)$$

Exchange

$$G_n + D_m \xrightarrow{k_e} D_n + G_m \ (n, m \geqslant 0)$$

$$Q_n + R_m \xrightarrow{k_e} R_n + Q_m \ (n, m \geqslant 0)$$

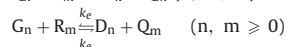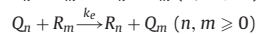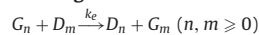$$G_n + R_m \underset{k_e}{\overset{k_e}{\rightleftharpoons}} D_n + Q_m \quad (n, \ m \geqslant 0)$$

The optimization reduces the batch time by 47% while meeting the same product quality constraints. This indicates a significant improvement over current operations.

To extend this process to integrated scheduling and dynamic optimization, we consider the unified time grid in Fig. 8. Here the discrete time representation is adopted to enable detailed modeling of process characteristics in both the scheduling and operation layers. In this figure, the entire scheduling time horizon is indexed by $t \in \{1, 2, \ldots, H\}$ with H discrete time slots of unit length. A time slot contains finite elements with collocation points inside each element. Also, note that the starting point of a scheduling time slot is aligned with a finite element, so that task switching events, represented as binary variables, are addressed simultaneously. Both the scheduling and dynamic modeling equations are then formulated as a nonconvex Mixed Integer Non-Linear Program (MINLP).
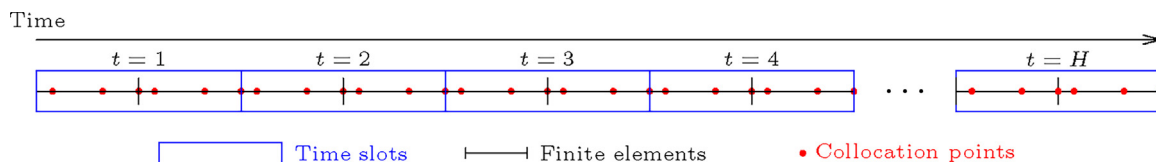
Fig. 8. Time representation of the integrated formulation.

5.2. Case study results

To demonstrate this integrated approach we consider the polyether polyol process model in Nie et al. (2015a,b). As shown in Fig. 9, the plant has two parallel polymerization reactors (Rxr1, Rxr2) of identical processing capacity; both connect to the downstream buffer tank (T) followed by the purification unit (PU). Three types of products are made from the process (A, B, C) with different specifications on molecular weight and byproduct ratio. An integrated approach is applied to maximize the overall profit of the process within a given scheduling horizon. As a result, rigorous dynamic models are developed for the polymerization reactors, while the other continuous units are modeled using the Resource Task Network (RTN) representation.

The two semi-batch reactors, Rxr1 and Rxr2, demand a large cooling capacity as reactions are highly exothermic. An interesting feature of the plant is that the two reactors share cooling utility from the same source. Moreover, the optimized schedule must produce a predetermined amount of Product A according to customer orders, while additional Product B and C can be made beyond ordered amounts. The decision variables are the task assignments for scheduling, and the control strategy of the reactors includes the temperature trajectory and monomer feed policy. There are two polymerization modes for Products B and C with the same quality specs but different task lengths; Product A has only one polymerization mode. PU has a maximum processing rate that is product dependent. Costs consist of cooling utility cost, fixed cost for polymerization operations and PU maintenance, and penalties for monomer flow rate and temperature fluctuations. The goal of the integrated optimization is to maximize the plant profit over a 3-day scheduling time horizon, which is calculated by product sales minus total manufacturing cost.

To determine the schedule, the RTN models materials and process unit availability as resources that can be generated and/or consumed by operating tasks. This model allocates tasks over time while ensuring that resource levels stay within feasible limits. Detailed derivation of the RTN model can be found in Nie et al. (2014). To illustrate this model, we describe the following resource balance equation, which accounts for the variation of excess resource levels over time.

$$R_{r,t} = R_{r,t-1} + \sum_{i \in \mathcal{I}} \sum_{m \in \mathcal{M}} \sum_{\theta=0}^{\tau_{i,m}} \mu_{i,m,r,\theta} \bar{w}_{i,m,t,\theta}$$
$$+ \sum_{i \in \mathcal{I}} \sum_{m \in \mathcal{M}} \sum_{n \in \mathcal{N}} \sum_{\theta=0}^{\tau_{i,m}} \nu_{i,m,n,r,\theta} \bar{\bar{\xi}}_{i,m,n,t,\theta} + \Pi_{r,t},$$
$$\forall r \in \mathcal{R}, t \in \mathcal{T}. \quad (5)$$
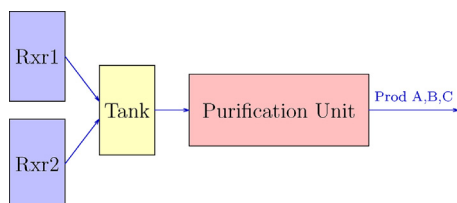

Fig. 9. Flowsheet of the polyether polyol process.

Here, R is the resource level, $\bar{w}$ and $\bar{\bar{\xi}}$ are the discrete and continuous task history states, τ is the task length, μ and ν are the corresponding task resource parameters, and Π is used to represent external transfer events. The subscripts are r for resource, t for time slot, i for tasks, m for task modes, n for task extents. Also, θ is a dummy subscript to account for time delay shifts in the resource balance. Analogous equations are also derived to represent the task history states ($\bar{w}, \bar{\bar{\xi}}$) as well as the upper and lower bounds of the resource levels and task histories.

The integrated formulation proposed in Nie et al. (2015a,b) ties the RTN scheduling model and process dynamic models together along the time line presented in Fig. 8. Task switching events are described by the task assignment/history variables in the RTN scheduling model. The integrated formulation for scheduling and dynamic optimization is given by:

$$\max \quad \underbrace{\Phi(R_{r,t}, z_t, y_t, u_t, \bar{w}_{i,m,t,\theta}, \bar{\bar{\xi}}_{i,m,n,t,\theta})}_{\text{Overall profit}}$$
$$= \underbrace{\Phi^{sch}(R_{r,t}, \bar{w}_{i,m,t,\theta}, \bar{\bar{\xi}}_{i,m,n,t,\theta})}_{\text{Product sales}}$$
$$- \underbrace{\Phi^{dyn}(z_t, y_t, u_t, \bar{w}_{i,m,t,\theta}, \bar{\bar{\xi}}_{i,m,n,t,\theta})}_{\text{Manufacturing cost}}$$

$s.t.$ Scheduling equations, analogous to Eq. (5)
$$F^{sch}(R_{r,t}, R_{r,t}^{\min}, R_{r,t}^{\max}, \bar{w}_{i,m,t,\theta}, \bar{\bar{\xi}}_{i,m,n,t,\theta}) = 0 \quad (6)$$

Scheduling inequalities, analogous to Eq. (5)
$$G^{sch}(R_{r,t}, R_{r,t}^{\min}, R_{r,t}^{\max}, \bar{w}_{i,m,t,\theta}, \bar{\bar{\xi}}_{i,m,n,t,\theta}) \leq 0$$

Dynamic equations
$$F^{dyn}(z_t, y_t, u_t, \bar{w}_{i,m,t,\theta}, \bar{\bar{\xi}}_{i,m,n,t,\theta}) = 0$$

Dynamic inequalities
$$G^{dyn}(z_t, y_t, u_t, \bar{w}_{i,m,t,\theta}, \bar{\bar{\xi}}_{i,m,n,t,\theta}) \leq 0$$

The overall objective function $\Phi(\cdot)$ is written as two subobjectives $\Phi^{sch}(\cdot)$ and $\Phi^{dyn}(\cdot)$ that depend on scheduling and dynamic optimization variables, respectively. Also, the constraints can be separated into scheduling and dynamic optimization groups.

The integrated MINLP formulation (6) is solved with Generalized Benders Decomposition (GBD). The scheduling equations (in master problem) and dynamic models (in primal problem) are linked only by the task history variables. The primal problem comprises the dynamic optimization to minimize manufacturing cost, with fixed complicating variables ($\bar{w}, \bar{\bar{\xi}}$). The master problem comprises the RTN scheduling model, a projection of the primal problem in the space of complicating variables, and cutting planes (Benders cuts) that bound $\Phi(\cdot)$ from below. Using GBD, the optimal solution of the original problem is bounded by the best primal (upper bound) and master problem (lower bound) solutions.

The GBD method applies an iterative procedure to obtain the optimal solution of the original problem, while the primal problem is solved in an inner loop and the relaxed master problem guides the selection of complicating decision variables. At first, the primal problem is solved with the complicating variables fixed at an initial point. The master problem is then solved to update the complicating variables, and trigger the next GBD iteration. As iterations proceed the best primal solution gives the upper bound of the opti-
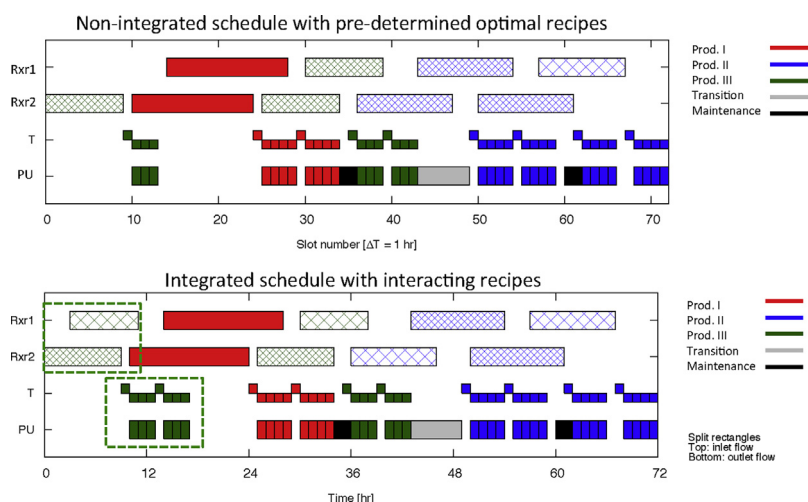
Fig. 10. Optimal production schedules without integration (above) and with integrated recipes. Note the highlighted batches allowed with the integrated approach.

mal objective value, while the relaxed master problem calculates the lower bound. As Benders cuts are accumulated in the master problem, the lower bound is non-decreasing through the iterations. The algorithm terminates when lower and upper bounds fall within optimality tolerances. On the other hand, global optimality can only be guaranteed when the primal problem is convex.

For the case study, the GBD algorithm solves the problem in only three iterations, due to the inclusion of the Benders cuts and the incorporation of the RTN scheduling problem in the GBD master. The MILP master problems, with over 28,700 continuous variables and 1825 binary variables, are solved in less than 10 CPU s. Primal NLP problems with 14,820 variables solve in less than 200 CPUs. Additional details on case study results and algorithm performance can be found in Nie et al. (2015a,b).

The optimal plant profit for the integrated optimization approach is 10.5% higher than the schedule determined with fixed, optimally generated recipes. Optimized schedules with and without integration are shown for both cases in Fig. 10. Task rectangles denote different products and task recipes. For the buffer tank (T), the upper small rectangles represent the material transfer operations that load the reactor products to the buffer tank, while the lower rectangles represent the outgoing flows from the tank (T) to the purification unit (PU). In addition, reactors Rxr1 and Rxr2 may be used as temporary storage units when the buffer tank is not immediately available. The PU processes different products, carries out transition cleaning, and turns offline for maintenance to replenish its processing capacity.

The non-integrated schedule in Fig. 10 produces two batches of Product A, four batches of Product B, and three batches of Product C. However, cooling utilities become too expensive when running two parallel batches of Product C with pre-determined recipes. On the other hand, for the integrated schedule, we note that an additional batch of Product C is produced. Here the dynamic optimization determines new interacting recipes for Rxr1 and Rxr2 that reduce utility costs and allow a profitable additional batch. Unfortunately, because the non-integrated approach uses fixed reactor recipes independent of the production schedule, it cannot consider these unit interactions.

The capability to update optimal reactor recipes at will leads to considerable flexibility in on-line scheduling. This was demonstrated in Nie et al. (2015a,b), where a similar dynamic recipe optimization model was deployed within an on-line scheduling system and coupled to the plant DCS. In a year-long series of plant trials, this capability led to a reduction in manual process interventions by 75%, a decrease in batch wait time by 50% and increased process productivity of 5%, translating to a gain of about 5×10^6/year.

6. Conclusions and future work

Strengthened by powerful optimization algorithms and modeling environments, simultaneous collocation has developed into an effective methodology for the systematic development and optimization of dynamic chemical processes. This study shows how these dynamic optimization strategies overcome a number of difficulties that present severe challenges with competing approaches.

This study considers three real-world chemical process systems that have been optimized with the simultaneous collocation approach. The first case is a singular optimal control problem with unstable dynamic modes that arise from an exothermic catalytic reaction. Simulation of these systems often leads to runaway behavior with unbounded profiles. The simultaneous collocation approach determines an optimal catalyst activity profile that leads to significant performance improvements in product yield as the number of catalytic zones increase. Moreover, simultaneous collocation is shown to approach the infinite dimensional, singular solution arbitrarily closely.

The second process example deals with grade transitions in the LLDPE process, where we describe a novel multi-stage approach based on product specification bands. This leads to a dynamic optimization formulation for a "set to set" transition, which is enabled by the simultaneous collocation approach. The resulting multi-stage formulation leads to over 30% reduction in off-grade product, when compared to the classical single stage optimization.

The third process example considers the determination of optimal recipes for a semi-batch polyol process. Since the main reactions are exothermic and reactor cooling is essential, typical operating recipes are heavily constrained and conservative. In contrast, simultaneous dynamic optimization solves this problem in less than a CPU minute and leads to feasible and safe operation with 47% less time. This detailed model can be embedded directly into a process scheduling scheme with the result that optimal schedules with detailed reactor performance can be determined during operation. This leads to a further 10% increase in profitability, when compared to the best fixed-recipe schedule.

These results demonstrate the significant gains that are due to solving dynamic optimization problems efficiently and reliably. They also illustrate the importance of applying more flexible problem formulations, advanced optimization modeling platforms

and efficient large-scale nonlinear programming solvers. These are essential tools that enable superior results.

Future research will be devoted to expanding these concepts and tools so that they can be applied more widely to larger and more challenging problems. As dynamic optimization models increase, NLP solvers and modeling environments require more efficiency and robustness. Moreover, continuous development of parallel computation and advanced computing architectures need to be leveraged to improve and redesign optimization strategies.

Moreover, optimal solutions presented here were determined for models developed under nominal conditions. On the other hand, there are many sources of uncertainty due to model mismatch, uncertain process parameters, measurement errors and equipment performance decay that compromise these optimal solutions. Such uncertainties can be built into the optimization problem so that feasible designs can be determined with superior performance characteristics. Advances in this area include large-scale algorithms applied to multi-scenario optimization as well as formulations for back-off constraints (Shi et al., 2016a,b; Srinivasan et al., 2003), Lucia et al. (2013), and Galvanin et al. (2010).

Finally, dynamic optimization solutions have their ultimate value when they can be deployed and validated on-line. This task requires the integration of on-line control with numerical optimization. Concepts to address this problem include stability and robustness of the implemented dynamic optimization, as well as efficient solution of "time critical", yet accurate process optimization models. Although these concepts are beyond the scope of this paper, they are explored in Yang et al. (2015), Biegler et al. (2015), Griffith et al. (2017) and have been demonstrated with preliminary on-line optimization results for the polyol polyether process in Jung et al. (2015) and Jang et al. (2016).

Acknowledgments

References

AIMMS, 2014. Advanced Interactive Multidimensional Modeling System, http://aimms.com/; https://en.wikipedia.org/wiki/AIMMS.

Arrieta-Camacho, J.J., Biegler, L.T., 2006. Real time optimal guidance of low-thrust spacecraft: an application of nonlinear model predictive control. Ann. N. Y. Acad. Sci. 1065, 174.

Ascher, U.M., Petzold, L.R., 1998. Computer Methods for Ordinary Differential Equations and Differential-Algebraic Equations. SIAM, Philadelphia, PA.

Barton, P.I., Allgor, R.J., Feehery, W.F., Galan, S., 1998. Dynamic optimization in a discontinuous world. Ind. Eng. Chem. Res. 37, 966–981.

Betts, J., 2010. Practical Methods for Optimal Control and Estimation Using Nonlinear Programming. SIAM Series on Advances in Design and Control 19. Philadelphia, PA, USA.

Betts, J.T., Campbell, S.L., 2003. Discretize Then Optimize. M&CT-TECH-03-01 Technical Report. The Boeing Company.

Bhatia, T., Biegler, L.T., 1996. Dynamic optimization in the design and scheduling of multiproduct batch plants. Ind. Eng. Chem. Res. 35, 2234–2246.

Biegler, L.T., 2010. Nonlinear Programming: Concepts, Algorithms and Applications to Chemical Processes. SIAM, Philadelphia.

Biegler, L.T., Yang, X., Fischer, G.G., 2015. Advances in sensitivity-based nonlinear model predictive control and dynamic real-time optimization. J. Process Control 30, 104–116.

Bliss, G.A., 1946. Lectures of the Calculus of Variations. University of Chicago Press, Chicago, IL.

Bock, H.G., 1983. Numerical treatment of inverse problem in differential and integral equations. In: Recent Advances in Parameter Identification Techniques for O.D.E. Springer, Heidelberg, Federal Republic of Germany.

Bock, H.G., Plitt, K.J., 1984. A multiple shooting algorithm for direct solution of optimal control problems. 9th IFAC World Congress, Budapest.

Boltyanskii, Y., Gamkrelidze, R., Pontryagin, L.S., 1956. On the Theory of Optimal Processes, vol. 110. Proc. USSR Academy of Sciences.

Brooke, A., Kendrick, D., Meeraus, A., Raman, R., 1998. GAMS – A User's Guide. http://www.gams.com.

Bryson, A.E., Ho, Y.C., 1975. Applied Optimal Control. Hemisphere.

Büskens, C., Maurer, H., 2001. Real-time control of an industrial robot. In: Grötschel, M., Krumke, S., Rambau, J. (Eds.), Online Optimization of Large Systems. Springer, Berlin, pp. 57–68.

Byrd, R.H., Gilbert, J.C., Nocedal, J., 2000. A trust region method based on interior point techniques for nonlinear programming. Math. Prog. 89, 149–185.

Chen, W., Biegler, L.T., 2016. Bilevel direct transcription optimization for singular optimal control problems. AIChE J. 62 (10), 3611–3627.

Courant, R., Hilbert, D., 1953. Methods of Mathematical Physics. Interscience Press, New York.

Cuthrell, J.E., Biegler, L.T., 1989. Simultaneous optimization and solution methods for batch reactor control profiles. Comput. Chem. Eng. 13, 49–62.

Drud, A., 1994. CONOPT – a large scale GRG code. ORSA J. Comput. 6, 207–216.

Flores-Tlacuahuac, A., Biegler, L.T., Saldivar-Guerra, E., 2005. Dynamic optimization of hips open-loop unstable polymerization reactors. I & EC Res. 44 (8), 2659–2674.

Fourer, R., Gay, D.M., Kernighan, B.W., 2002. AMPL: A Modeling Language for Mathematical Programming. Duxbury Press/Brooks/Cole Publishing Company.

Galvanin, F., Barolo, M., Bezzo, F., Macchietto, S., 2010. A backoff strategy for model-based experiment design under parametric uncertainty. AIChE J. 56 (8), 2088–2102.

Griffith, D.W., Zavala, V.M., Biegler, L.T., 2017. Robustly stable economic NMPC for non-dissipative stage costs. J. Process Control 57, 116–126.

Hager, W.W., 2000. Runge–Kutta methods in optimal control and the transformed adjoint system. Numer. Math. 87, 247–282.

Hart, W., Laird, C., Watson, J.-P., Woodruff, D.L., 2012. Pyomo: Optimization Modeling in Python. Springer, Berlin.

Jang, H., Lee, J.H., Biegler, L.T., 2016. A robust NMPC scheme for semi-batch polymerization reactors. IFAC Pap. Online 49 (7), 37–42.

Jung, T.-Y., Nie, Y., Lee, J.H., Biegler, L.T., 2015. Model-based on-line optimization framework for semi-batch polymerization reactors. IFAC-PapersOnLine 48 (8), 164–169.

Kameswaran, S., Biegler, L.T., 2008a. Convergence rates for direct transcription of optimal control problems using collocation at Radau points. Comput. Optim. Appl. 41 (1), 81–126.

Kameswaran, S., Biegler, L.T., 2008b. Advantages of a nonlinear programming based methodologies for inequality path constrained optimal control problems – a numerical study. SIAM J. Sci. Comput. 30 (2), 957–981.

Leineweber, D.B., 1999. Efficient Reduced SQP Methods for the Optimization of Chemical Processes Described by Large Sparse DAE Models. University of Heidelberg, Heidelberg, Germany.

Lucia, S., Finkler, T., Engell, S., 2013. Multi-stage nonlinear model predictive control applied to a semi-batch polymerization reactor under uncertainty. J. Process Control 23 (9), 1306–1319.

Nie, Y., Biegler, L.T., Villa, C.M., Wassick, J.M., 2013a. Reactor modeling and recipe optimization of polyether polyol processes: polypropylene glycol. AIChE J. 59 (7), 2515–2529.

Nie, Y., Witt, P., Agarwal, A., Biegler, L.T., 2013b. Optimal active catalyst and inert distribution in catalytic fixed bed reactors: ortho-xylene oxidation. I&EC Res. 52 (44), 15311–15320.

Nie, Y., Biegler, L.T., Villa, C.M., Wassick, J.M., 2014. Extended discrete-time resource task network formulation for the reactive scheduling of a mixed batch/continuous process. I & EC Res. 53 (44), 17112–17123.

Nie, Y., Biegler, L.T., Villa, C.M., Wassick, J.M., 2015a. Discrete time formulation for the integration of scheduling and dynamic optimization. I&EC Res. 54 (16), 4303–4315.

Nie, Y., Lin, B., Hayot, P., Wassick, J.M., et al., 2015b. Dynamic real-time optimization of a mixed mode process. Presented at Annual AIChE Meeting, Salt Lake City.

Nyström, R., Franke, R., Harjunkoski, I., Kroll, A., 2005. Production campaign planning including grade transition sequencing and dynamic optimization. Comput. Chem. Eng. 29, 2163–2179.

Pontryagin, V.V., Boltyanskii, Y., Gamkrelidze, R., Mishchenko, E., 1962. The Mathematical Theory of Optimal Processes. Interscience Publishers Inc., New York, NY.

Raghunathan, A.U., Gopal, V., Subramanian, D., Biegler, L.T., Samad, T., 2004. Dynamic optimization strategies for three-dimensional conflict resolution of multiple aircraft. AIAA J. Guidance Control Dyn. 27, 586–594.

Ray, W.H., 1981. Advanced Process Control. McGraw-Hill, New York.

Shi, J., Biegler, L.T., Hamdan, I., 2016a. Optimization of grade transitions in polyethylene solution polymerization process under uncertainty. Comput. Chem. Eng. 95, 260–279.

Shi, J., Biegler, L.T., Hamdan, I., 2016b. Optimization of grade transitions in polyethylene solution polymerization processes. AIChE J. 62 (4), 1126–1142.

Srinivasan, B., Bonvin, D., Visser, E., Palanki, S., 2003. Dynamic optimization of batch processes: II. Role of measurements in handling uncertainty. Comput. Chem. Eng. 27 (1), 27–44.

Steinbach, M.C., Georg Bock, H., Kostin, G.V., Longman, R.W., 1997. Mathematical optimization in robotics: towards automated high speed motion planning. Math. Ind. 7, 303–340.

Vassiliadis, V.S., Sargent, R.W.H., Pantelides, C.C., 1994a. Solution of a class of multistage dynamic optimization problems. Part I – Algorithmic framework. Ind. Eng. Chem. Res. 33, 2115–2123.

Vassiliadis, V.S., Sargent, R.W.H., Pantelides, C.C., 1994b. Solution of a class of multistage dynamic optimization problems. Part II – Problems with path constraints. Ind. Eng. Chem. Res. 33, 2123–2133.

Wächter, A., Biegler, L.T., 2006. On the implementation of a primal-dual interior point filter line search algorithm for large-scale nonlinear programming. Math. Program. 106 (1), 25–57.

Yang, X., Griffith, D.W., Biegler, L.T., 2015. Nonlinear programming properties for stable and robust NMPC, Proc. 5th IFAC Conference on Nonlinear Model Predictive Control. IFAC-PapersOnLine 48 (23), 388–397.